

Decomposition and activation of Pt-dendrimer nanocomposites on a silica support

D. Samuel Deutsch¹, Gwendoline Lafaye¹, Dongxia Liu¹, Bert Chandler², Christopher T. Williams^{1,*}, and Michael D. Amiridis^{1,*}

¹Department of Chemical Engineering, University of South Carolina, Columbia, SC 29208

²Department of Chemistry, Trinity University, San Antonio, TX 78212

Received 28 April 2004; accepted June 21, 2004

Zero valent platinum nanoparticles were stabilized in solution by the use of poly(amido)amine dendrimers and were subsequently deposited onto a porous silica support. The resulting materials were subjected to various thermal treatments in oxidizing, reducing, and inert environments, in order to remove the surrounding polymer and expose the Pt metal sites to gas phase reagents. The materials were characterized at several different stages during this process via Fourier-Transform Infrared (FTIR) spectroscopy and Transmission Electron Microscopy (TEM). The results suggest that the dendrimer decomposition occurs at its mono-substituted amide groups and begins at relatively low temperatures (~50 °C). The presence of oxygen in the gas phase and the Pt particles in the Pt-dendrimer nanocomposite accelerate this process. Oxidation at 425 °C was the most successful temperature for removing the dendrimer fragments from the Pt surface, rendering the Pt sites most accessible for carbon monoxide adsorption. Limited sintering of the Pt particles is observed under these conditions, as well as during subsequent reduction steps, necessary to yield the metallic form of Pt.

KEY WORDS: poly(amido)amine; dendrimer; platinum; supported catalysts.

1. Introduction

Conventional catalyst preparation methods utilizing inorganic salt precursors, such as incipient wetness impregnation or co-precipitation, attempt to control the final morphology of supported metal particles by optimizing precursor solution conditions and time-temperature profiles of subsequent calcinations/reduction steps. However, these methods have only limited success, generally yielding a wide distribution of metal particle sizes and providing little control over particle composition and morphology [1].

The use of dendrimers, a family of hyper-branched, spherical polymers, may offer a unique path to rational design and synthesis of nanostructured heterogeneous catalysts. Crooks *et al.* [2] showed that dendrimers can be used to control the size, stability, and solubility of nanoparticles in solution. The diameters of such dendrimer-stabilized nanoparticles range from 1 to 4 nm. In particular, poly(amido)amine (PAMAM) dendrimers can exchange metal ions into their branches. Subsequent reduction in solution yields dendrimer-stabilized semiconductor [3] or metallic [4–7] nanoparticles. Crooks and co-workers have also demonstrated the activity of dendrimer-stabilized metallic nanoparticles in homogeneous catalysis [7] and heterogeneous electrocatalysis [6]. So far, only limited information is available regarding the use of dendrimer-stabilized metal nanoparticles

for the synthesis of heterogeneous catalysts [8–11]. Velarde-Ortiz and Larsen [9] have deposited CuO nanoparticles stabilized by fifth-generation poly(propylene)imine dendrimers on a silica sol-gel matrix. The presence of copper was found to catalyze the oxidative removal of the host dendrimer resulting in a potentially catalytically active material. Lang *et al.* [10] have used fifth-generation, hydroxyl-terminated (G5OH) PAMAM dendrimer-encapsulated platinum nanoparticles to synthesize a silica supported catalyst. Characterization results of this study showed that the resulting catalyst has a narrower particle size distribution than what is observed with a traditionally impregnated platinum catalyst on the same SiO₂ support and with the same Pt loading. After removal of the dendrimer, oxidation of carbon monoxide and toluene hydrogenation were demonstrated. Most recently, Lafaye *et al.* [11] have reported that PAMAM G4OH dendrimer-stabilized ruthenium nanoparticles can be used to synthesize Ru/Al₂O₃ catalysts with a mean particle size of 2.0 nm and a narrow particle size distribution after removal of the dendrimer shell. Once again, this catalyst compares favorably to one synthesized via a wet-impregnation procedure.

The goal of this paper is to further explore the conditions necessary to decompose and remove hydroxyl-terminated PAMAM dendrimers from the surface of supported catalysts. We have synthesized PAMAM G4OH-stabilized Pt nanoparticles in solution, deposited the dendrimer-metal nanocomposites onto a silica

*To whom correspondence should be addressed.

E-mail: willia84@engr.sc.edu; amiridis@engr.sc.edu

support, and exposed the resulting material to several thermal treatments. The decomposition of the dendrimer component was monitored during these treatments *in situ* via Fourier-Transform Infrared (FTIR) spectroscopy. Furthermore, FTIR spectroscopy of adsorbed CO was used to investigate the accessibility of the active platinum sites after various oxidation and reduction treatments. Combined with particle size data from Transmission Electron Microscopy (TEM) measurements, the results suggest that the structure of the resulting catalyst is dependent on the oxidation and reduction temperatures, as well as treatment time.

2. Experimental approach

2.1. Synthesis

Zerovalent Pt-dendrimer nanocomposites were prepared following the method developed by Crooks *et al.* [4]. Fourth-generation hydroxyl-terminated poly(amido)amine (G4OH-PAMAM) starburst dendrimers in methanol were obtained from Aldrich. The methanol was removed via a rotovap and the solution was diluted to 0.1 mM G4OH with deionized water. About 50 mL of 4.0 mM $K_2[PtCl_4]$ solution was mixed with 50 mL of 0.1 mM G4OH, yielding a Pt to dendrimer ratio of 40:1, and was allowed to react for 3 days. G4OH-PAMAM dendrimers have 62 available sites for metal ion coordination. A ratio of 40 Pt atoms per dendrimer was chosen to allow for equilibrium dispersion of the ion precursor throughout the dendrimers. $K_2[PtCl_4]$ was used as received from Aldrich. The resulting Pt^{2+} -G4OH solution was subsequently reduced at room temperature with flowing hydrogen (National Welders) and strongly stirred for approximately 1 h. Finally, the samples were dialyzed for 2 days at room temperature to remove any remaining impurities (10 mm \times 6 mm cellulose membrane, Sigma-Aldrich).

Supported catalyst samples were prepared by wet-impregnation of the resulting Pt-G4OH solution onto a silica support (Grace-Davison Sylopol 948). Prior to impregnation, the support was calcined for 12 h at 500 °C in air. The water in the Pt-G4OH/silica solution was allowed to evaporate by stirring for 2 days in a chemical hood. The dried Pt-G4OH/SiO₂ catalyst had a Pt loading of 0.9 wt% (measured by atomic absorption spectroscopy).

2.2. Characterization

A Hitachi H8000 TEM was used to obtain micrographs of unsupported dendrimer stabilized Pt nanoparticles (nanocomposites), silica supported nanocomposites, and Pt nanoparticles after dendrimer removal. In preparation for imaging, approximately 15 mg of the supported catalyst was finely crushed and dispersed in 3 mL of deionized water by ultrasonifica-

tion for 15 min. A drop of this fine dispersion was deposited on a Cu grid and was allowed to sit for 5–10 min. Similarly, a drop of the Pt-G4OH solution was used to image particles prior to impregnation. Excess liquid was removed with absorbent filter paper before inserting the sample grid into the instrument. Images were typically obtained at magnifications of 500,000–700,000 \times with a voltage of 200-kV supplied to the electron gun. Particle size distributions were obtained by measuring the diameters of no less than 100 metal particles in at least two micrographs of each sample.

FTIR spectra of the catalyst in the gas phase were collected in the single beam absorbance mode with a resolution of 2 cm⁻¹, using a Nicolet Nexus 470 spectrometer equipped with a MCT-B detector. A 10 cm-long water-cooled stainless steel IR flow cell with NaCl windows was used to hold a catalyst wafer of 12 mm diameter and thickness of approximately 5.0 mg/cm². A heating element wrapped around the cell allowed for various heat treatments and collection of *in situ* spectra at different temperatures. Total gas flowrates were maintained at \sim 70 mL/min. The cell temperature was monitored by a thermocouple placed in close proximity to the catalyst sample.

During the dendrimer decomposition studies, *in situ* spectra were collected either in flowing He or a 50% O₂–50% He mixture. The temperature was raised in a step-wise manner (steps of 50 °C) from room temperature to 400 °C. Several spectra were collected at each temperature, until a steady state was reached. Only then, was the next temperature increase applied. During the catalyst activation studies, each sample was exposed to an oxidizing environment (50% O₂–50% He mixture) followed by a reducing environment (100% H₂). The temperature and duration of the oxidation and reduction treatments were varied during different experiments. The sample was then cooled back to room temperature in flowing He and a background spectrum was recorded. Next, a 1% CO–99% He mixture was flowed over the catalyst for 15 min, followed by a purge by pure He for an additional 15 min. Spectra were collected every 2 min from the start of CO flow until the end of the 30-min period.

3. Results and discussion

3.1. Pt-G4OH nanocomposites

The majority of Pt particles in the aqueous Pt-G4OH nanocomposite solution (\sim 90%) were observed by TEM to have diameters in the 2.0–5.0 nm range with an average of 3.4 ± 1 nm. Following impregnation of the Pt-G4OH nanocomposites onto a porous silica support and partial drying at room temperature, an average particle size of 4.0 ± 1 nm was observed, indicating that the impregnation process slightly increases the average Pt particle size. The observed

particle sizes suggest that the predominant method of nanoparticle formation in this case is by arrested precipitation (as opposed to templating within the dendrimer), where several G4OH dendrimers stabilize a Pt particle, as reported by Pellechia and co-workers [12]. More recent studies in our laboratory have demonstrated that nanoparticles (including bimetallic particles) with much smaller diameters and tighter size distributions can be obtained with slight modification of the synthetic parameters, and subsequently may be delivered with minimal sintering to catalyst supports.

The partially dried Pt-G4OH/SiO₂ material was also exposed to gas phase CO at room temperature. FTIR spectra in this case indicated no adsorption of CO onto Pt, suggesting that the Pt sites are not accessible. Results of H₂ chemisorption measurements conducted in parallel also indicated no significant uptake of hydrogen by platinum in the partially dried Pt-G4OH/SiO₂ material. In contrast, results of previous catalytic studies conducted by Crooks et al. [2,13] have shown that Pd and Pt sites are accessible to small molecules when Pt-G4OH or Pd-G4OH nanocomposites are studied in solution. In fact, they show substantial catalytic activity and selectivity for hydrogenation reactions [2,13]. Consequently, it appears that during drying of the Pt-G4OH/SiO₂ material, the dendrimer collapses onto the Pt particles rendering them inaccessible to gas phase molecules. This phenomenon has also been observed by Chandler and co-workers for silica-supported Pt-G5OH [10]. A similar behavior was also observed with Pt-G4OH nanocomposites supported on γ -alumina. Attenuated total reflection infrared (ATR-IR) studies revealed that, while the nanoparticles are accessible to CO in the liquid phase, no adsorption occurred when the material was dry [14].

3.2. Dendrimer decomposition studies

The partially dried Pt-G4OH/SiO₂ material was subsequently subjected to a number of different thermal and chemical treatments with the goal of decomposing the dendrimer component and exposing the Pt sites. FTIR spectra collected during treatment of the Pt-G4OH/SiO₂ sample with flowing helium or a 50% O₂–50% He mixture at different temperatures are shown in figures 1 and 2, respectively. The background spectra for these experiments were recorded with the dried material at room temperature; accordingly, negative peaks represent species modified on, or removed from, the catalyst surface. The readily observable broad band centered at approximately 1550 cm⁻¹ can be assigned to the C–N stretching and C–N–H bending vibrations of the amide group in the dendrimer's structure. Furthermore, the stretching vibration of the dendrimer's amide C=O bond occurs in the 1630–1680 cm⁻¹ region [15–20]. However, in the spectra of figures 1 and 2 this broad band is partially masked by the strong water band in the

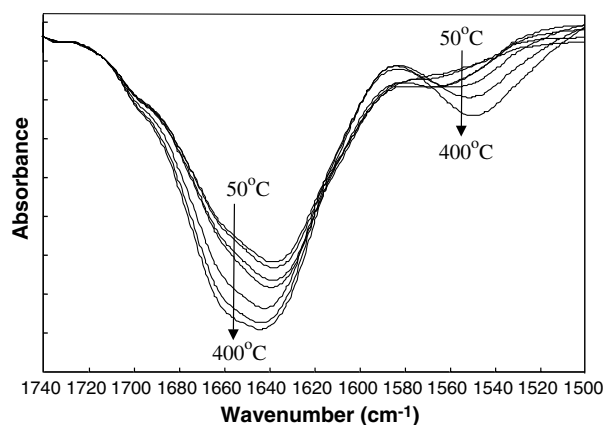


Figure 1. *In situ* spectra of Pt-G4OH/SiO₂ collected at 50 °C intervals in flowing He. (From the top spectrum, the spectra were collected at 50, 100, 150, 200, 250, 300, 350, and 400 °C).

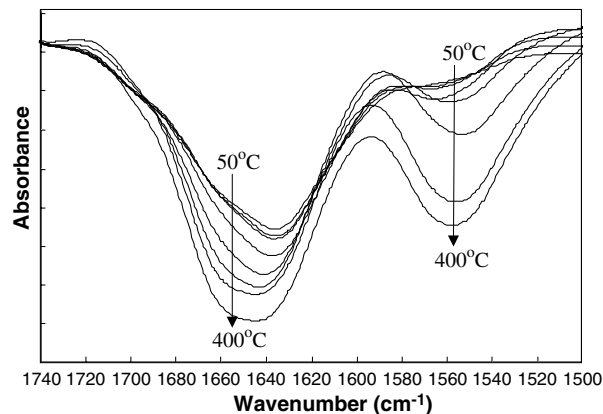


Figure 2. *In situ* spectra of Pt-G4OH/SiO₂ collected at 50 °C intervals in a flowing 50% O₂–50% He mixture. (From the top spectrum, the spectra were collected at 50, 100, 150, 200, 250, 300, 350, and 400 °C).

same region, since substantial amounts of water are still present in the partially dried Pt-G4OH/SiO₂ sample.

The spectra of figures 1 and 2 display the progressive decomposition of the dendrimer component at elevated temperatures and the oxidation/desorption of the decomposed amide groups from the silica surface. Furthermore, a comparison between the two sets of spectra indicates that the presence of O₂ accelerates the dendrimer decomposition/desorption process. This is more clearly observed by comparing the intensities of each of the bands at 1550 cm⁻¹, where the water interference is not present.

The decomposition of the dendrimer in the Pt-G4OH/SiO₂ material was also compared to the decomposition of the same dendrimer in a non-platinated G4OH/SiO₂ sample. The two samples were prepared via identical methods. Spectra of the two samples collected at 400 °C in a flowing 50% O₂–50% He mixture are shown in Figure 3. The results show a much higher intensity of the negative dendrimer peaks in the

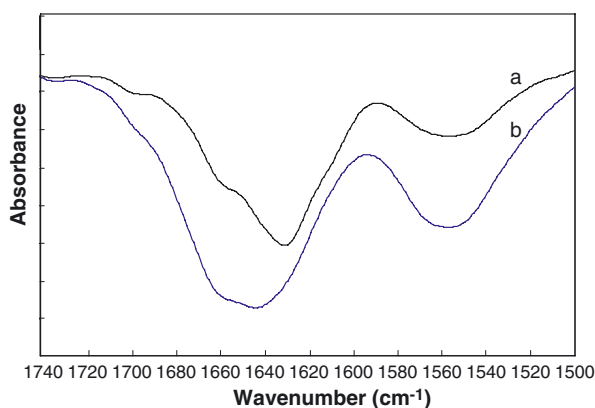


Figure 3. *In situ* spectra of G4OH/SiO₂ (a) and Pt-G4OH/SiO₂ (b) samples, collected at 400 °C in a flowing 50% O₂–50% He mixture.

platinated sample, suggesting that platinum catalyzes the dendrimer oxidation/decomposition process.

3.3. Catalyst activation studies

A series of experiments were conducted next to determine the optimum conditions for catalyst “activation.” We explored a set of oxidation/reduction steps that would eventually yield zero-valent metallic Pt particles capable of chemisorbing CO. As noted earlier, exposure of the partially dried Pt-G4OH/SiO₂ catalyst to a 1% CO–99% He mixture resulted in no significant uptake of CO. Similarly, additional drying for 1 h at 100 °C in flowing He did not result in any CO uptake either, suggesting further that the Pt sites are not simply “flooded” covered” by the dendrimer shell.

Spectra of adsorbed CO, collected at room temperature following oxidation of the Pt-G4OH/SiO₂ sample at different temperatures and subsequent reduction in flowing hydrogen for 1 h at 200 °C, are shown in figure 4. The strong characteristic IR peak observed in all cases in the 2060–2085 cm^{−1} range can be assigned to CO linearly bonded on Pt. This peak exhibits substantial tailing towards lower wavenumbers, suggesting the presence of a distribution of Pt sites with respect to the strength of CO adsorption. These variations in wavenumber may also be in part due to the presence of the dendrimer or its remnants. The sample oxidized at 425 °C also shows some degree of bridge-bonded CO, as indicated by the presence of the broad peak in the 1800–1850 cm^{−1} region. The intensities of the peaks in the 2080 cm^{−1} region further indicate that the amount of chemisorbed CO increases with increasing oxidation temperature up to 425 °C. The results of similar experiments conducted with a variable time of oxidation at 425 °C (figure 5), indicate that an oxidation period longer than 1 h slightly decreases the amount of chemisorbed CO. These results suggest that the decomposition/desorption of the dendrimer is complete after 1 hour of oxidation at 425 °C, and further exposure to this temperature leads to a small degree of sintering.

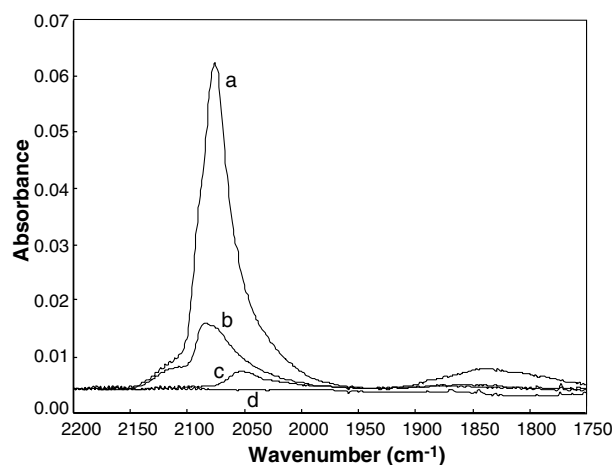


Figure 4. Room temperature FTIR spectra of adsorbed CO on Pt-G4OH/SiO₂ following oxidation at (a) 425 °C, (b) 350 °C, and (c) 275 °C for 1 h and subsequent reduction at 200 °C for 1 h. The sample labeled (d) was treated only in a He environment for 1 h at 100 °C.

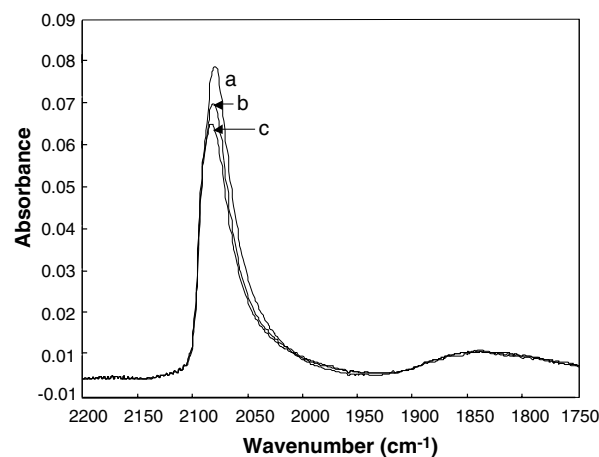


Figure 5. Room temperature FTIR spectra of adsorbed CO on Pt-G4OH/SiO₂ following oxidation of the sample at 425 °C for (a) 1 h, (b) 2 h, and (c) 4 h, and subsequent reduction at 200 °C for 1 h.

The effect of the H₂ reduction temperature on the CO chemisorption capacity of the catalyst was examined next. The results are shown in figure 6 and suggest that a temperature of 200 °C is sufficient for the full reduction of the catalyst. Any further increase in reduction temperature leads to a decrease in CO adsorption capacity, indicating that sintering of the Pt metal particles is initiated in this temperature range under reducing conditions. The appearance of the wide, low-intensity bridge-bonded CO bands in spectra (b) and (c) of figure 6 further supports this conclusion.

Results of TEM analyses are in accord with these FTIR measurements. The average platinum particle size increases from 4.0 ± 1 to 4.1 ± 2 and 4.4 ± 2 nm, for the untreated catalyst, the catalyst reduced at 200 °C, and the catalyst reduced at 400 °C, respectively. These results suggest that while the 425 °C oxidation 200 °C

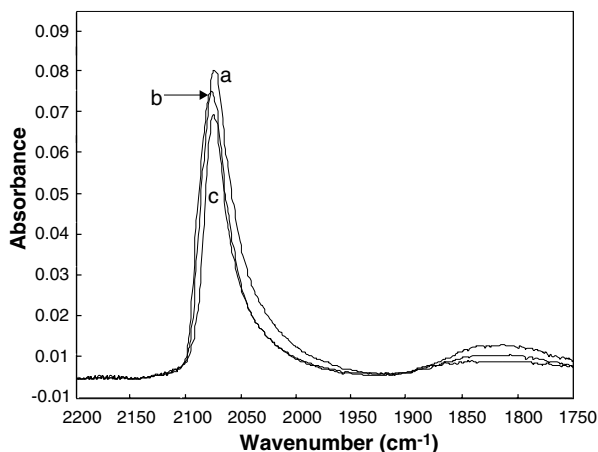


Figure 6. Room temperature FTIR spectra of adsorbed CO on Pt-G4OH/SiO₂ following oxidation of the sample at 425 °C for 1 h and subsequent reduction at (a) 200 °C, (b) 300 °C, and (c) 400 °C for 1 h.

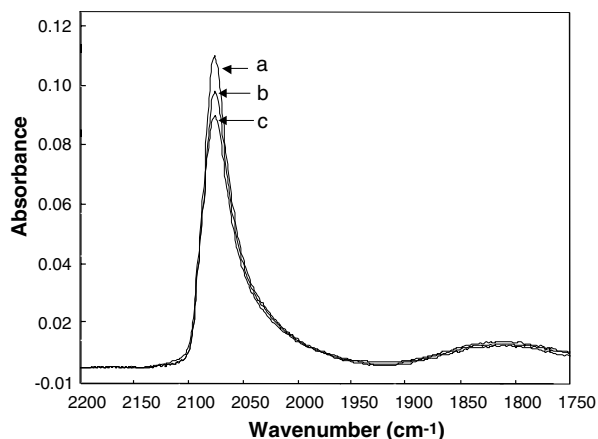


Figure 7. Room temperature FTIR spectra of adsorbed CO on the Pt-G4OH/SiO₂ catalyst following oxidation of the sample at 425 °C for 1 h and subsequent reduction at 200 °C for (a) 1 h, (b) 2 h, and (c) 4 h.

reduction sequence does not significantly affect the particle size distribution, an increase of the reduction temperature to 400 °C results in limited sintering.

Lastly, we investigated the effect of reduction time at 200 °C. The spectra of adsorbed CO collected with these samples are shown in figure 7 and indicate that an increase in reduction time at this temperature leads to a decrease in the CO adsorption capacity of the catalyst, once again through the sintering of the Pt nanoparticles. No substantial change was observed in this case in the intensity of the bridge bonded CO band at approximately 1800 cm⁻¹.

4. Conclusions

The goal of this study was to characterize the decomposition and activation of supported dendrimer-derived Pt nanoparticles in order to obtain a procedure

that will remove the surrounding dendrimer component and expose the maximum number of Pt sites for catalysis. Pt-G4OH nanocomposites were deposited by standard wet-impregnation onto a porous silica support with minimal metal agglomeration, suggesting that this is a viable delivery protocol onto the support. Results from dendrimer decomposition studies suggest that the decomposition/desorption of Pt-G4OH/SiO₂ begins at temperatures as low as 50 °C and continues up to 425 °C. Both an oxidizing environment and the presence of platinum significantly accelerate this decomposition/desorption process. Zero valent platinum metal particles can be obtained if the dendrimer decomposition/oxidation process is followed by a reduction step at a temperature of 200 °C. Reduction at higher temperatures leads to limited sintering and a slight increase in metal particle size.

Acknowledgments

The authors wish to acknowledge the National Science Foundation (NSF Award CTS-0103135) for financial support of this work. DSD further expresses his gratitude to the Alfred P. Sloan Foundation and the University of South Carolina African American Professors Program. Finally, GL expresses her gratitude to the French Government for the support provided through the Lavoisier Postdoctoral grant.

References

- [1] G. Ertl, H. Knozinger and J. Weitkamp, *Handbook of Heterogeneous Catalysis* (VCH, Weinheim, 1997).
- [2] R.M. Crooks, M. Zhao, L. Sun, V. Chechik and L.K. Yeung, *Acc. Chem. Res.* 34 (2001) 181.
- [3] K. Sooklal, L.H. Hanus, H.J. Ploehn and C.J. Murphy, *Adv. Mater.* 10 (1998) 1083.
- [4] R.M. Crooks, M. Zhao and L.J. Sun, *J. Am. Chem. Soc.* 120 (1998) 4877.
- [5] D. Tomalia and L.A. Balogh, *J. Am. Chem. Soc.* 120 (1998) 7355.
- [6] R.M. Crooks and M. Zhao, *Adv. Mater.* 11 (1999) 217.
- [7] Y. Niu and R.M. Crooks, *Chem. Mater.* 15 (2003) 3463.
- [8] R.M. Crooks and L. Sun, *Langmuir* 18 (21) (2002) 8233.
- [9] R. Velarde-Ortiz and G. Larsen, *Chem. Mater.* 14 (2002) 858.
- [10] H. Lang, R. Alan May, B.L. Iversen and B.D. Chandler, *J. Am. Chem. Soc.* 125 (2003) 14832.
- [11] G. Lafaye, C.T. Williams and M.D. Amiridis, *Catal. Lett.* 96 (2004) 43.
- [12] P.J. Pellechia, J. Gao, Y. Gu, H.J. Ploehn and C.J. Murphy, *Inorg. Chem.* 43 (4) (2004) 1421.
- [13] Y. Niu, L.K. Yeung and R.M. Crooks, *J. Am. Chem. Soc.* 123 (28) (2001) 6840.
- [14] D. Liu, J. Gao, C.J. Murphy and C.T. Williams, *J. Phys. Chem. B* submitted. Please update
- [15] I. Suzuki, *Bull. Chem. Soc. Jpn.* 35 (1962) 540.
- [16] T.J. Mizazawa, *Chem. Phys.* 29 (1958) 611.
- [17] T.J. Mizazawa, *Chem. Phys.* 24 (1956) 408.
- [18] R.D.S. Fraser and W.C. Price, *Nature (London)* 170 (1952) 490.
- [19] C.G. Cannon, *Spectrochim. Acta.* 16 (1960) 302.
- [20] M. Beer, H.B. Kessler and G.B.B.M. Sutherland, *J. Chem. Phys.* 29 (1958) 1097.